TITLE:

Quantitative reverse transcription PCR assay to detect pyrethroid resistance in *Culex* mosquitoes

Authors: Kelli M. Hager [1,2,6], Erick Gaona[1], Amy Kistler [3], Kalani Ratnasiri [3], Hanna Retallack [4], Miguel Barretto [1], Sarah S. Wheeler [6], Christopher M. Hoover [2] Eric J. Haas-Stapleton [1*]

Affiliations:

[1] Alameda County Mosquito Abatement District, Hayward, CA 94545

[2] University of California, Berkeley, School of Public Health, Berkeley, CA 94720

[3] Chan Zuckerberg Biohub, San Francisco, CA 94158

[4] University of California, San Francisco, CA 94158

[5] Sacramento-Yolo County Mosquito and Vector Control District, Elk Grove, CA 95624

[6] Currently: New York State Department of Public Health, Wadsworth Center, Empire State Plasa, Albany, NY 12237

*Corresponding author: Eric.Haas@mosquitoes.org

Key words: Culex, kdr, pyrethroid resistance, assay

Abstract

Pyrethroid insecticides are widely used to control mosquitoes that transmit diseases such as West Nile virus (WNV) to humans. A single nucleotide polymorphism (SNP) in the knockdown resistance locus (*kdr*) of the *voltage gated sodium channel* (*Vgsc*) gene of *Culex* mosquitoes confers knockdown resistance to pyrethroids. PCR-based assays that detect these SNPs in *Culex* species are currently available for *Culex pipiens* Linnaeus and *Culex quinquefasciatus* Say. RNAseq was employed to sequence the coding region of *Vgsc* for *Culex tarsalis* Coquillett and *Culex erythrothorax* Dyar, two WNV vectors. We utilized the cDNA sequence to develop a quantitative reverse transcriptase PCR assay that detects the L1014F mutation in the *kdr* of V*gsc*. Because this locus is conserved, the assay successfully detected the SNPs in multiple *Culex spp.* vectors of WNV in the United States. The resulting *Culex* RT*kdr* assay was validated using quantitative PCR, CDC bottle bioassays, and sequencing of PCR products. Using sequencing, we determined the accuracy of the *Culex* RT*kdr* assay was 99%. Pyrethroid resistance was more common among *Cx. pipiens* than other *Culex* spp. and co-occured with agriculture. We anticipate that public health and vector control agencies may utilize the *Culex* RT*kdr* assay to map the distribution of pyrethroid resistance in *Culex* species to more efficiently control mosquitoes and the diseases they transmit.

Introduction

Many mosquitoes within the *Culex* genus that are present in California are vectors for diseases caused by West Nile virus (WNV), St. Louis Encephalitis virus (SLEV), and filarial worms [1]. WNV and SLEV are maintained in a bird-mosquito cycle by mosquitoes such as *Culex pipiens* Linneaus and *Culex erythrothorax* Dyar that preferentially feed on birds. *Culex tarsalis* Coquillett, another WNV vector, transition seasonally from ornithophilic to general feeders or when host availability is constrained [2, 3]. Humans and horses are considered dead-end hosts for these arboviruses because they generate low viremia, thereby preventing onward transmission of these arboviruses [4, 5]. There have been over 6,700 symptomatic human infections of WNV since it was introduced to California in 2003 [6, 7]. Vector control agencies interrupt disease transmission through environmental manipulation, biological or chemical control of adult and juvenile mosquitoes, and public education. Adulticides (pesticides that target biting adult mosquitoes) are used to reduce mosquito abundance and the transmission of pathogens.

Pyrethroid adulticides preferentially bind to open voltage gated sodium channels (*Vgsc*) in neuronal membranes, preventing their closure. The open *Vgsc* leaves the membrane depolarized and the neuron unable to transmit signals among cells, resulting in paralysis (i.e. knockdown) and death of the insect [8, 9]. More than 50 mutations in the sodium channel gene are associated with pyrethroid resistance among arthropods [10].

The most common among *Culex* species is the L1014F single nucleotide polymorphism (SNP), which promotes closed state inactivation and knockdown resistance [11, 12].

Pyrethroids are commonly used to control structural and agricultural arthropod pests. The CDC considers mosquito populations resistant to an adulticide when knockdown or mortality rates are less than 80% in an adult mosquito bottle bioassay (BBA; [13]). Increased use of pyrethroids in agricultural settings may contribute to pyrethroid resistance among a broad range of arthropods [14] [15]. Concerns with widespread pyrethroid resistance in mosquitoes prompted us to develop a quantitative reverse transcriptase-PCR (qRT-PCR) assay that detects the L1014F SNP in *Culex* species. Our original goal was to develop this assay for use in *Culex tarsalis*, but after comparing the cDNA sequences of other *Culex* vectors we discovered the qRT-PCR assay produced a more conserved template compared to its qPCR counterparts. Here we describe the development of a *Culex* RT*kdr* assay and an application of the assay to map pyrethroid resistance within Alameda County (California, USA).

Methods

1. Mosquito Collection

Adult mosquitoes used for RT*kdr* testing were collected overnight from May - October of 2019 in Alameda County (California, USA) using Encephalitis Vector Survey traps (BioQuip, Rancho Dominguez, CA) that were baited with dry ice. A scientific collection

92 permit was not required because the collections were made by a mosquito abatement
93 district that was operating under the legislative authority of the California Health and
94 Safety Code § 2040. The field studies did not involve endangered or protected species.
95
96 Collected mosquitoes were identified to species using a dissection microscope and chill
97 table (BioQuip, Rancho Dominguez, CA). Individual whole mosquitoes were placed into
98 2 ml microcentrifuge bead mill tubes that contained 2.8 mm ceramic beads (Fisher
99 Scientific, Waltham, MA) and frozen at -20^{o}C until use. Susceptible *Cx. tarsalis* utilized
100 in insecticide CDC bottle bioassays described below were from the Kern National
101 Wildlife Refuge (KNWR) colony [16, 17] and resistant *Cx. tarsalis* maintained in an
102 insectary that were originally collected during 2019 in Woodland, California USA
103 (Conaway strain; GPS coordinates: 38.647287, -121.668173). These strains were also
104 used in the *Culex* RT*kdr* assay as controls for susceptible (wildtype KNWR strain) or
105 resistant (mutant Conaway strain) *Cx. tarsalis*.
106
107 *2. RNA Extraction*
108
109 Individual whole mosquitoes were homogenized in 200 µl of MagMAX Lysis/Binding
110 Buffer that was diluted 1:2 in phosphate buffer saline for 45 s using a Fisherbrand Bead
111 Mill 24 Homogenizer (Thermo Fisher Scientific, Waltham, MA). RNA was extracted
112 using the MagMAX-96 Viral RNA Isolation Kit and KingFisher Duo Prime Purification
113 System programed with the MagMAX Pathogen Standard Volume software protocol as
114 described by the manufacturer (Thermo Fisher Scientific, Waltham, MA) with the

following exceptions: 80 µl of homogenate was extracted, magnetic beads were washed with 250 µl of wash solution, and the RNA was eluted in 50 µl. Notably, we employed the same method to extract RNA from mosquitoes that is widely used when testing for the presence of arboviruses [18]. Alternatively, RNeasy Plus Mini Kits (Qiagen, Mississauga, Ontario, Canada) were used to extract RNA from mosquitoes, as recommended by the manufacturer (Qiagen, Mississauga, Ontario, Canada). RNA concentration in the samples was measured using a NanoDrop 2000 Spectrophotometer (ThermoFisher Scientific, Waltham, MA) according the manufacturer recommendations.

3. RNAseq of *Vgsc* gene

Vgsc sequences were recovered from the host fraction of a metatranscriptomic RNAseq dataset derived from total RNA extracted from *Cx. erythrothorax* (N = 44) and *Cx. tarsalis* (N = 26) single mosquitoes collected from across California [19]. Sample collection, total RNA extraction, and paired-end mNGS RNAseq from each of the single mosquito specimens that served as input data here are described elsewhere ([19]; Sequence related archive: https://www.ncbi.nlm.nih.gov/sra/PRJNA605178). Raw fastq R1 and R2 data from each mosquito were first compressed to a unique set of reads sharing < 95% sequence identity via CD-HIT software [20, 21]. Translated blastx alignment of the resulting R1 and R2 reads with a representative *Vgsc* protein sequence from *Culex quinquefasciatus* Say (NCBI protein accession AFW98419.1; [22] was applied to identify deduplicated R1 and R2 reads from each mosquito sample which

showed ≥50% of their length aligned with ≥90% identity to the *Cx. quinquefasciatus Vgsc* reference sequence. Seqtk software (https://github.com/lh3/seqtk) was used to compile the separate *Culex erythrothorax* and *Cx. tarsalis* fastq reads that met these criteria from the 44 *Cx. erythrothorax* or 26 *Cx. tarsalis* individually deduplicated datasets. Partners of unpaired reads included in each pool were identified and included to ensure a full complement of paired reads, including additional potentially divergent *Vgsc* sequences that were not captured in the alignment step.

A total of 410 *Culex tarsalis* input read pairs and 481 *Culex erythrothorax* read pairs were carried forward from this step. Trimmomatic software [23] was used to remove the Sequencing library adapter sequences, along with low quality terminal bases of the reads. The resulting paired-end pooled datasets were each then separately used as input for SPAdes [24] paired-end *de novo* assembly of *Vgsc* transcripts. To facilitate *Vgsc* contig coverage analysis, read pools were aligned back to each of the identified *Vgsc* contigs via Bowtie2 [25].

The *Cx. tarsalis* and *Cx. erythrothorax* contig assemblies were aligned to the NCBI nt and nr databases via blastn and blastx, respectively, to identify the set of *de novo* assembled contigs that corresponded to *Vgsc* transcripts. A single 6878 bp *Cx. tarsalis* contig and two 6364 bp and 506 bp *Cx. erythrothorax* contigs were identified for further analyses. The *Cx. tarsalis* 6878bp contig encompasses an uninterrupted 2113 amino acid open reading frame, with additional 5’ 321 bp and 3’ 218 bp flanking terminal sequences.

The most closely related sequences in NCBI to this contig corresponded to several *Culex* complete *Vgsc* nucleotide and protein coding sequences. The best match was the *Cx. pipiens pallens* strain SS sodium channel mRNA (NCBI accession numbers KY171978.1 and ARO72116.1), showing ≥95% overall sequence identity at both the nucleotide and amino acid level. The *Cx. erythrothorax* contigs were not joined in the initial de novo assembly; however, the blastn and blastx alignment termini indicated a short (< 10 bp) region of overlapping sequence at the ends of these 2 contigs. Manual joining of these 2 contigs generated a 6709 bp contig that encodes an uninterrupted open reading frame of 2109 amino acids, and additional flanking 283 bp of 5'utr and 99 bp of 3'utr sequences. The best match is the *Cx. quinquefasciatus* isolate S-Lab sodium channel mRNA, complete cds (NCBI accession numbers EU817515.1 and ARO72116.1), showing ≥95% overall sequence identity at both the nucleotide and amino acid level. Accession numbers for the recovered *Cx. erythrothorax* and *Cx. tarsalis Vgsc* transcript sequences are MW176091 and MW176090, respectively. Resulting assemblies were manually reviewed via Geneious software (version 2019.0.4; https://www.geneious.com/) to generate final contig consensus sequences.

4. Detection of kdr SNP by RT-PCR

The primer and probe sequences to detect the *kdr* SNP were designed using Primer3Plus software (Table 1; [26]) based on the cDNA of *Vgsc* from *Cx. tarsalis* and *Cx. erythrothorax* (GenBank No. MW176090 and MW176091, respectively). Wildtype

and mutant probes were labeled with fluorescein (FAM) and hexachlorofluorescein (HEX), respectively (Integrated DNA Technologies, Coralville, Iowa). A diagram depicting primer and probe locations, the 1014 mutation and intron site for *Vgsc* of *Cx. tarsalis* is provided in Figure 1. Nucleotide sequences were aligned using Basic Local Alignment Search Tool [27].

Table 1. Primers and probes used in the *Culex* RT*kdr* assay. Red text indicates the location of the *kdr* SNP.

Name	Sequence (5' → 3')
Primers	
RTSeq_Fwd	ATCTGACGTTTGTGCTCTGC
RT*kdr*_Fwd	CCTGCATTCCGTTCTTCTTG
RT*kdr*_Rev	GCGATCTTGTTCGTTTCGTT
Probes	
RT*kdr*_WT	FAM-GGTTAAGTA/ZEN/CGACTAAGTTTCCTATCACTAC-3IABkFQ
RT*kdr*_Mutant	HEX-GGTTAAGTA/ZEN/CGACAAAGTTTCCTATCACTAC-3IABkFQ

The Taqman Fast Virus 1-Step Master Mix (Thermo Fisher Scientific, Waltham, MA) was prepared as described by the manufacturer using 1 µl of template RNA (48.8-144.8

ng/µl), primers diluted to 900 nM and probes diluted to 250 nM. PCR plates were vortexed for 10 s at the highest setting (Fisherbrand™ Analog Vortex Mixer, ThermoFisher Scientific, Waltham, MA), centrifuged for 15 seconds (MPS 1000 Mini PCR Plate Spinner, Labnet International, Inc., Edison, NJ) and subsequently analyzed with a QuantStudio™ 5 Real-Time PCR System (Thermo Fisher Scientific, Waltham, MA) using the Genotyping setting which assigns sample results based on a proprietary algorithm. Amplification curves were reviewed manually to ensure algorithm accuracy. RT-qPCR cycling conditions were as follows: 50°C for 5 minutes, 95°C for 20 seconds, followed by 40 cycles of 95°C for 3 seconds and 60°C for 30 seconds. Primer and probe concentration and PCR cycling conditions were optimized to discriminate homozygous and heterozygous genotypes. Allele controls were added in the form of a no template control and a known susceptible control for *Cx. tarsalis*, *Cx. pipiens* and *Cx. erythrothorax*. A known resistant control was also included for each of the former except *Cx. erythrothorax* because a resistant specimen of that species was not found in the current study.

5. Validation Methods

5.1 Insecticide Susceptibility Assays

CDC bottle bioassays were conducted to evaluate the resistance of adult mosquitoes to insecticides, according to CDC guidelines [13]. Three replicate bottles were evenly coated with 1 ml of technical grade insecticide (43 µg permethrin or 22 µg deltamethrin)

that was diluted in acetone. Control bottles contained only acetone diluent. The diluent was evaporated from the bottles in the dark at room temperature. Adult female mosquitoes were transferred to the bottles (14-23 mosquitoes per bottle), and the number of dead or knocked down mosquitoes was recorded at 15 min intervals for 180 min. A mosquito was recorded as dead or knocked down if it could not stand unaided when the bottle was gently rotated; otherwise, the mosquito was counted as alive. Live and dead mosquitoes were separated, tested with the *Culex* RT*kdr* assay and the PCR products sequenced. Resistance ratios were calculated using the proportion of dead mosquitoes at the 45 min time point when average mortality was less than 100% with those from the susceptible Conway strain in the denominator.

5.2 Validating the Culex RTkdr assay using Cx. pipiens quantitative PCR (qPCR) Taqman assay

The *Cx. pipiens* quantitative PCR (qPCR) Taqman assay that was developed previously [28] was used to validate the *Culex* RT*kdr* assay using *Cx. pipiens* samples. We followed the protocol for Taqman Multiplex Master Mix (ThermoFisher Scientific, Waltham, MA) with the following exceptions: BSA was excluded and nucleic acid that was isolated with the MagMAX-96 Viral RNA Isolation Kit (described above) was used as the template. We evaluated 75 *Cx. pipiens* mosquitoes using both the Taqman qPCR and *Culex* RT*kdr* assay and results were compared. Discordant samples were evaluated by sequencing the PCR products.

241 *5.3 Sequencing of PCR Products*

242

243 PCR products were submitted to Elim Biopharmaceuticals (Hayward, CA) for PCR
244 cleanup and sequencing. Because the RT*kdr*_Fwd primer is in close proximity to the
245 SNP, we designed a sequencing primer further upstream in the *Cx. tarsalis* mRNA
246 sequence that produced a 373 bp PCR product (RTseq_Fwd, Figure 1, Table 1).
247 Primer, probe and template concentrations and PCR cycling conditions to generate
248 PCR products for sequencing were as described above. Sequences were aligned to the
249 *tarsalis Vgsc* mRNA sequence using MUSCLE [29] to locate the *kdr* SNP.
250 Chromatograms were examined using 4Peaks software (Nucleobytes, Amsterdam, The
251 Netherlands) to determine if heterozygosity was present at the SNP site.

252

253 *6. Analyzing the Geographic Distribution of the kdr SNP*

254

255 Tableau Software (Seattle, WA) was used to map the geographic distribution of the *kdr*
256 SNP in mosquitoes that were collected in Alameda County (CA, USA). Allelic data for
257 mosquitoes that were collected within 1 km of each other were combined. The trap sites
258 were binned into two geographic regions, bayside and inland, that are separated by the
259 San Francisco East Bay Hills, a natural boundary that limits movement of mosquitoes
260 between the two regions. The distribution of allelic frequency was assessed by
261 mosquito species and by geographical region (inland and bayside) within Alameda
262 County. The resistant allele frequency, F_R, in each population was estimated (Equation

263 1) where $2N_{RR}$ is the number of homozygous resistant mosquitoes, N_{RS} is the number of
264 heterozygous resistant and N is the mosquito population size.
265
266 Equation 1. Equation for calculating resistance allele frequency
267 $F_R = (2N_{RR} + N_{RS}) / 2N$
268
269 Associations between genotype, Y, and mosquito species, region of collection, and area
270 type surrounding the collection site were estimated using Equation 2 from an ordinal
271 logistic regression model with ordered outcome categories (SS, RS, RR). The model
272 was fit using the polr function from the MASS [30] package in R Software (version
273 3.5.0;[31]) and used to estimate unadjusted and adjusted odds ratios for each variable.
274 Figures were generated using ggplot2 software [32].
275
276 Equation 2. Equation for ordinal logistic regression model
277 $\text{Logit}\,(P\,(Y \leq j)\,) = \beta_{0j} - \beta_1\text{Species} - \beta_2\text{Region} - \beta_3\text{AreaType}$
278
279 **Results & Discussion**
280
281 *1. Sequence Alignments*
282
283 The *Vgsc* -1 cDNA sequences for *Cx. tarsalis* (GenBank No. MW176090), *Cx.*
284 *erythrothorax* (GenBank No. MW176091) and *Cx. pipiens* (GenBank No. KY171978;
285 [33]) were aligned using BLAST. There was 95.7% identity with the greatest divergence

coming from the *Cx. pipiens* sequence. The forward and reverse primers matched 100% for all three species, however there were two mismatched nucleotides in the probe for *Cx. pipiens* (Figure 2, red boxes). These mismatches in *Cx. pipiens* resulted in less RT-PCR product relative to *Cx. tarsalis* and *Cx. erythrothorax* and no cross amplification of the wildtype and mutant RT-PCR probes as was observed for *Cx. tarsalis* and *Cx. erythrothorax* (Figure 3).

2. Interpreting RT-PCR Results

Increased FAM or HEX fluorescence indicated a homozygous wildtype or mutant genotype, respectively (Figures 3A, 3C, 3D, 3F). A similar quantity of FAM and HEX fluorescence indicated that the specimen had a heterozygous genotype (Figures 3B, 3E). Allelic discrimination plots for *Cx. pipiens* and *Cx. tarsalis,* respectively, were used to identify outliers (Figure 4). Performance of the assay was also assessed using ΔCT values between the two probes as described below.

The ΔCT values for both *Cx. tarsalis* and *Cx. pipiens* were analyzed to determine a cutoff value for homozygous and heterozygous samples. For *Cx. tarsalis* the average ΔCT value of the heterozygous genotype was 0.264 ± 0.238 with a range of 0.008 – 0.932. Based on this information, *Cx. tarsalis* samples with a ΔCT of <1 were considered heterozygous. The average ΔCT values for mutant homozygous *Cx. tarsalis* was 2.944 ± 0.413 with a range of 2.077 – 3.964 and an average of 3.107 ± 0.782 with a range of 2.044 – 6.593 for homozygous wildtype. Therefore, samples with ΔCT

values >2 were considered homozygous. ΔCT values for *Cx. erythrothorax* resembled *Cx. tarsalis* for homozygous wildtype, and was the only genotype detected for that species. Heterozygous ΔCT values were used to determine the *Cx. pipiens* genotypes because the opposing probes did not typically cross amplify for homozygous samples. Rarely, the opposing probe in *Cx. pipiens* samples amplified to produce a large ΔCT value. The average ΔCT of heterozygous *Cx. pipiens* samples was 0.981 ± 0.396 with a range of 0.164 – 1.779. Based on these findings, *Cx. pipiens* samples with ΔCT values under 2 were considered heterozygous and samples with undetermined or extremely large ΔCT values were considered homozygous.

Atypical amplification curves were occasionally observed for *Cx. pipiens* samples (< 5% of total), suggesting these mosquitoes may have been misidentified and were instead *Cx. erythrothorax*. *Culex pipiens* and *Cx. erythrothorax* are morphologically similar and can be mistaken for each other [4]. To help determine if the *Cx. pipiens* with uncharacteristic amplification curves may have been misidentified, we tested them using the *Cx. pipiens* qPCR assay that only produces a PCR product using nucleic acid isolated from *Cx. pipiens* or *Cx. quinquefasciatus* [28]. Each of those samples failed to amplify a product on the *Cx. pipiens* qPCR assay, providing additional evidence that the mosquitoes may have indeed been *Cx. erythrothorax*. *Culex tarsalis, Cx. pipiens, and Cx. erythrothorax* were the most prevalent *Culex* species collected during the study period. We also tested *Culex stigmatosoma* Dyar and *Culex apicalis* Adams. The low sample size for these species did not allow us to generate average ΔCT values. However, the amplification curves and sequenced PCR products were similar to *Cx.*

pipiens or *Cx. tarsalis* (Figure S1), suggesting the *Culex* RT*kdr* assay may be effective for those species as well.

3. Validation Results

3.1 Insecticide Susceptibility Assays

CDC bottle bioassays were used to identify *Cx. tarsalis* that were resistant or susceptible to permethrin and deltamethrin. Two lab-reared strains of *Cx. tarsalis* were assessed; one with known sensitivity to pyrethroids (KNWR strain) and another that displayed resistance (Conaway strain). The *Culex* RT*kdr* assay was used subsequently to determine the *kdr* SNP genotype of Conaway strain mosquitoes that were assessed in the bottle bioassay. Mortality or knockdown was on average less than 5% in mosquitoes placed in bottles that contained only diluent. At the 60 min time point, all susceptible strain (KNWR) mosquitoes had succumbed to permethrin and deltamethrin (Figure 5). At the 45 min time point, when the average mortality was less than 100% for all treatments, the Conaway strain was 54.5- and 58.8-fold more resistant to permethrin and deltamethrin, respectively. Resistance ratios of these magnitudes indicate that the Conaway strain was highly resistant to the insecticides. At 180 min, 21 ± 4% of the resistant Conaway strain mosquitoes had succumbed to permethrin and 38 ± 9% to deltamethrin (Figure 5). The slopes of the linear regression lines were significantly different for the Conway and KNWR strains (permethrin: $F_{(1,50)} = 309.2$, $P < 0.001$; deltamethrin: $F_{(1,50)} = 50.84$, $P < 0.001$), suggesting that their biological responses to

the insecticides were different. The World Health Organization (WHO) classifies a population as resistant when mortality is below 90% [34]. The higher mortality rate observed in deltamethrin is expected as deltamethrin is a type II pyrethroid. Permethrin, a type I pyrethroid, may be more effective at knockdown because type I pyrethroids dissociate from the target faster than type II [12]. Because type II compounds, like deltamethrin, remain bound to the target longer, they are more effective at killing insects.

The genotype at the *kdr* SNP of the Conaway strain mosquitoes that survived or succumbed to permethrin or deltamethrin in the bottle bioassays was determined using the *Culex* RT*kdr* assay. All of the mosquitoes that survived exposure to permethrin or deltamethrin were homozygous mutant at the *kdr* SNP. Although the heterozygous, mutant and wildtype genotypes were observed only in mosquitoes that succumbed to the insecticides, there was no significant difference in the distribution of the genotypes in the bottle bioassays (Permethrin: $F(2,2) = 18.21$, $P = 0.0521$; Deltamethrin: $F(2,2) = 5.569$, $P = 0.1522$). Genotype results from the *Culex* RT*kdr* assay were confirmed by sequencing PCR products and viewing chromatograms. Chromatograms revealed a second *kdr* mutation at the 1014 amino acid among the resistant Conaway strain (Figure 6). Of the 47 BBA Conaway mosquitoes sequenced, 6 (13%) were heterozygous for the phenylalanine and serine *kdr* mutations. Both mutations were previously described in *Cx. quinquefasciatus* [35]. The serine *kdr* mutation may be associated with cross-resistance between DDT and pyrethroids [35]. Because DDT persists in the environment [36], it may have exerted a selective pressure on

mosquitoes in the Conaway rice field that contributed to propagating the serine *kdr* mutation.

3.2 Culex pipiens kdr detection Taqman qPCR

To determine the fidelity of the *Culex* RT*kdr* assay, individual *Cx. pipiens* mosquitoes were evaluated with both the *Culex* RT*kdr* and the *Cx. pipiens* qPCR assays (N = 75 mosquitoes). Three specimens (4%) failed to amplify a product after 30 PCR cycles in the *Culex* RT*kdr* assay and were excluded. Of the remaining mosquitoes, 69/72 (96%) results were concordant across both assays. Discordant results were sequenced to determine the correct genotypic call. Chromatograms for the three (4%) discordant samples indicated the mosquitoes were heterozygous and in agreement with the *Culex* RT*kdr* results, demonstrating that the *Culex* RT*kdr* assay was highly accurate (Table 2; paired t test, P > 0.9999).

Table 2. Validating the *Culex* RT*kdr* assay using a *Cx. pipiens* qPCR Taqman assay

N	*Culex* RT*kdr* Assay			*Cx. pipiens* qPCR Assay		
	TTA (SS)	TTA/T (RS)	TTT (RR)	TTA (SS)	TTA/T (RS)	TTT (RR)
72	23	26	23	23	23	26

Susceptible homozygous (SS) TTA SNP, Heterozygous (RS) TTA/T SNP, Resistant homozygous (RR) TTT SNP

397

398 *4.3 Sequencing*

399

400 PCR products from the *Culex* RT*kdr* assay were sequenced to further assess assay
401 fidelity across five *Culex* species (N = 170; Table 3). Greater than 99% (169 out of 170)
402 of the specimens were concordant with the sequencing and *Culex* RT*kdr* assay results
403 (Table 3). The single discordant sample was misidentified as homozygous mutant by
404 the *Culex* RT*kdr* assay, but the chromatogram revealed two peaks at the SNP location,
405 indicating the mosquito was heterozygous (not shown). Using the sequencing results as
406 the "true" result, we found the accuracy of the *Culex* RT*kdr* assay to be greater than
407 99%. High accuracy is common among both qPCR and qRT-PCR assays [37, 38].
408 Among the mosquitoes that were collected in Alameda County, only the L1014F
409 mutation was found.

410

411 Table 3. Validating the *Culex* RT*kdr* assay by sequencing the resulting PCR products

Species (N)	RT-PCR			Sequencing		
	TTA (SS)	TTA/T (RS)	TTT (RR)	TTA (SS)	TTA/T (RS)	TTT (RR)
Cx. pipiens (51)	17	13	21	17	13	21
Cx. tarsalis (97)	18	17	62	18	18	61
Cx. erythrothorax (16)	16	0	0	16	0	0

Cx. stigmatosoma (5)	5	0	0	5	0	0
Cx. apicalis (1)	0	0	1	0	0	1
Total (170)	56	30	84	56	31	83

412

413 *5. Distribution of Pyrethroid Resistance*

414

415 The *Culex* RT*kdr* assay was used to assess the geographic distribution of the L1014F
416 *kdr* mutation in Alameda County (Figure 7). Among the individual *Culex spp.* that were
417 tested, 26.2% were homozygous resistant, 20.6% were heterozygous, and 53.3% were
418 homozygous susceptible (N = 1383 mosquitoes). Ordinal logistic regression was used
419 to determine associations between genotype, mosquito species, region of collection and
420 area type. Because no resistance was identified in *Cx. erythrothorax*, ordinal logistic
421 regression models were fit only to *Cx. pipiens* and *Cx. tarsalis* data. Table 4
422 summarizes the statistical results examining allele frequency and odds of resistant
423 genotypes (heterozygous and homozygous resistant). The overall resistant allele
424 frequency (F_R) was highest among *Cx. pipiens* (0.57), low for *Cx. tarsalis* (0.15) and not
425 present for *Cx. erythrothorax* (0.00). *Culex pipiens* had 8.99 times greater odds of
426 being heterozygous or homozygous resistant compared to *Cx. tarsalis* (Table 4, 95%CI:
427 6.96 - 11.69). Adjusting for region and area type increased the association between
428 resistance and *Cx. pipiens* (Table 4; OR: 11.01 (8.36 - 14.63)). The inland region
429 revealed a higher F_R compared to the bayside region for both *Cx pipiens* and *Cx.*

tarsalis (Figure 8). *Culex erythrothorax* was not present the inland region during the study period and all bayside *Cx. erythrothorax* were homozygous susceptible.

High resistant allelic frequencies were found previously in *Cx. pipiens* complex mosquitoes [11] [39]. *Culex erythrothorax* reproduce in heavily vegetated regions of shallow ponds and can be highly abundant in marsh habitats [40, 41]. While *Cx. erythrothorax* were typically found in bayside wetlands, *Cx. pipiens* and *Cx. tarsalis* were both present inland, yet the *Cx. pipiens* were far more resistant. Previous studies of urban creeks and outfall of storm drains in California found high levels of pyrethroids. The pyrethroids were proposed to have originated from homeowner use or structural pest control [20, 42]. Sites that were not near agriculture occasionally contained comparable levels of pyrethroids to those found in creeks near agricultural sites. The high levels of pyrethroids found in the sediments of the outfalls of storm drains may contribute to the resistance that we observed in *Cx. pipiens* as they reproduce in and around storm drain and storm drain outfalls [5, 43].

Table 4. Genotypes detected, F_R, unadjusted and adjusted odds rations among species, geographical region and land area type.

Variable		Genotype			Odds Ratio, OR (95% CI)		
	N	SS	SR	RR	F_R	Unadjusted	Adjusted
Species							
Cx. erythrothorax	126	126	0	0	0	NA	NA
Cx. tarsalis	507	401	57	49	0.15	Ref	Ref
Cx. pipiens	744	208	226	310	0.57	8.99 (6.98 - 11.69)	11.01 (8.36-14.63)

Region							
Bayside	744	519	136	89	0.21	Ref	Ref
Inland	633	216	147	270	0.54	3.92 (3.15 - 4.89)	4.89 (3.79 - 6.33)
Area Type							
Wildlife	484	296	94	94	0.29	Ref	Ref
Urban	306	123	81	102	0.47	1.95 (1.47 - 2.58)	0.96 (0.70 - 1.32)
Industrial	449	251	83	115	0.35	1.13 (0.87 - 1.46)	0.77 (0.57 - 1.03)
Agriculture	144	66	27	51	0.45	1.74 (1.21 - 2.53)	0.89 (0.58 - 1.37)

Homozygous susceptible (SS), heterozygous (RS), homozygous resistant (RR)

Mosquitoes from inland regions of Alameda County had elevated odds of containing the *kdr* SNP that is associated with pyrethroid resistance (Table 4; OR: 3.92 (3.15 - 4.89)). Adjusting for species and area type increased the association between resistance and mosquitoes that were collected from inland sites (OR: 4.89 (3.79 - 6.33)), suggesting an association present between inland mosquitoes and higher levels of resistance. The California Pesticide Information Portal (CPIP) shows that the top uses of pyrethroids in Alameda County were for structural pest control, wine grapes, almonds, pistachios and brussels sprouts (https://calpip.cdpr.ca.gov/main.cfm). While CPIP does not specify the township for structural pest control, using CPIP in conjunction with Pesticide Use Report (PUR) data, we were able to narrow agricultural pesticide use down to several locations within the inland region of Alameda County. Agriculture is widely practiced within the inland region of Alameda County and is less common in the bayside region. Studies of *Anopheles gambiae* suggest that insecticides from agriculture likely contribute to

462 resistance in *Anopheles gambiae*, the malaria mosquito [21, 44, 45]. A similar pattern of
463 pyrethroid use in agriculture cooccurring with pyrethroid resistance was observed in *Cx.*
464 *pipiens* and *Cx. tarsalis*, two important vectors of WNV in North America.
465
466 **Conclusion**
467
468 We developed a simple to use RT-qPCR assay that detects the *kdr* SNP that is
469 associated with resistance to pyrethroid insecticides in at least five *Culex spp.* of
470 mosquito. Like all PCR-based assays, the *Culex* RT*kdr* assay is not without limitations.
471 It assay does not detect the serine *kdr* mutation that was discovered by sequencing the
472 RT*kdr* assay PCR product from the Conaway strain (Figure 6). The serine *kdr* mutation
473 suggests prior selective pressures, possibly from historical applications of pyrethroids or
474 DDT. The *Culex* RT*kdr* assay also does not account for other pyrethroid resistance
475 mechanisms such as overexpression or mutation of CYP9M10. Overexpression of
476 CYP9M10 allows for increased detoxification of pyrethroids by cytochrome P450s
477 monooxygenases [5, 46]. It was extensively validated for only *Cx. pipiens*, Cx. *tarsalis*
478 and *Cx. erythrothorax* mosquitoes as we had a limited number of other *Culex* species
479 available for the study. However, preliminary results suggest the assay performs for *Cx.*
480 *apicalis* and *Cx. stigmatosoma*. Lastly, we know the assay performs well using Northern
481 California mosquitoes, but genetic diversity across different countries may prevent the
482 assay from detecting the L1014F mutation in these *Culex* species worldwide. More
483 research is needed to determine whether this assay could be applied to mosquitoes
484 collected outside of California.

Despite public health pesticide applications accounting for <1% of statewide pesticide use between 1993-2007 and with Alameda County Mosquito Abatement District having applied less than 300 ml of adulticide in the decade covering 2010 to 2020, pyrethroid resistance remains a concern [47]. Commercial use of insecticides for both structural and agricultural pest control may contribute to the higher pyrethroid resistance in mosquitoes from the inland region. In countries that ceased pyrethroid applications by vector control agencies, resistance remained high, likely due to household insecticides that contain pyrethroids [48].

The ability of the *Culex* RT*kdr* assay to perform well with multiple *Culex* species may benefit vector control agencies. It may be possible to apply this technique to other mosquito species as the V*gsc* sequences of *Aedes aeypti* Linnaeus and *Aedes albopictus* Skuse revealed a high percent identity around the V1016G *kdr* mutation, suggesting the development of an *Aedes* qRT-PCR assay may be possible [38]. Application of pyrethroids to a resistant population can potentially drive heterozygous populations (RS) to the homozygous resistant genotype (RR) further concentrates the and releases unnecessary chemicals into the environment. Prior to the development of this *Culex* RT*kdr*, there was no quantitative PCR assay to detect the L1014F mutation in *Cx. tarsalis*. The development of our *Culex* RT*kdr* assay satiates the need for a simple and reliable *Cx. tarsalis* PCR pyrethroid-resistance detection assay. We hope the assay will improve testing for pyrethroid resistance among *Culex* species.

FIGURE LEGENDS

Figure 1. Schematic representation of sequencing primer (cyan), PCR primers (yellow), probes (red and blue), SNP and the intron of the kdr loci in *Vgsc* for *Cx. tarsalis*.

Figure 2. Basic Local Alignment comparing *Cx. tarsalis* (Query, Genbank No. MW176090) to *Cx. pipiens* (Subject, Genbank No. KY171978). Yellow boxes denote location of forward and reverse primers, purple box denotes probe location and red are mismatched bases.

Figure 3. Amplification plots (ΔRN vs Cycle Number) with the wildtype probe labeled in blue and mutant probe in red. **(A)** *Culex pipiens* homozygous wildtype **(B)** *Culex pipiens* heterozygous **(C)** *Culex pipiens* homozygous mutant (**D)** *Culex tarsalis* homozygous wildtype (**E)** *Culex tarsalis* heterozygous **(F)** *Culex tarsalis* homozygous mutant.

Figure 4. Allelic discrimination plots (Wildtype RN vs Mutant RN) for **(A)** *Culex pipiens* and **(B)** *Culex tarsalis.* Homozygous mutants are labeled with red ellipses, heterozygous with yellow ellipses, and homozygous wildtype are labeled with blue ellipses. Homozygous controls are labeled as open squares, outlined in their respective color. No template controls are labeled as black squares.

Figure 5. Bottle bioassay. Permethrin BBA results are depicted with closed squares with either blue or red representing permethrin susceptible or permethrin resistant, respectively. Deltamethrin BBA results are shown with open circles with either light blue or pink representing deltamethrin susceptible or deltamethrin resistant, respectively. Deltamethrin graphs are offset by 2 minutes for clarity. Equation of lines: Deltamethrin: susceptible KNWR strain, $Y = 1.785*X - 6.627$ ($R^2 = 0.7403$); resistant Conaway strain, $Y = 0.2499*X - 6.805$ ($R^2 = 0.5130$); Permethrin: susceptible KNWR strain, $Y = 1.818*X - 1.553$ ($R^2 = 0.9283$); resistant Conaway strain, $Y = 0.1337*X - 3.682$ ($R^2 = 0.6443$)

Figure 6. Chromatogram depicting heterozygosity for both the phenylalanine and serine/*kdr* mutations at the 1014 amino acid.

Figure 7. Resistance mapping within Alameda County showing **(A)** *Culex pipiens* and **(B)** *Culex tarsalis* in bayside and inland regions.

Figure 8. Resistant allele frequency (F_R) of the L1014F *kdr* mutation by species and region. Bright blue, dark blue and medium blue bars represent F_R for *Cx. erythrothorax* (no resistance detected), *Cx. pipiens* and *Cx. tarsalis*, respectively. The F_R for bayside *Cx. pipiens* and *Cx. tarsalis* was 0.375 ± 0.018 and 0.0840 ± 0.012, respectively. The F_R for inland *Cx pipiens* and *Cx. tarsalis* was 0.749 ± 0.016 and 0.230 ± 0.016, respectively.

Figure S1. *Culex* RT*kdr* assay amplification curves for **(A)** *Cx. stigmatosoma* (N = 3, each was heterozygous) and **(B)** *Cx. apicalis* (N = 3, two were homozygous mutant, one was heterozygous,).

REFERENCES

1. Farajollahi A, Fonseca DM, Kramer LD, Kilpatrick AM. "BIRD BITING" MOSQUITOES AND HUMAN DISEASE: A REVIEW OF THE ROLE OF CULEX PIPIENS COMPLEX MOSQUITOES IN EPIDEMIOLOGY. Infect Genet Evol. 2011;11(7):1577-85. doi: 10.1016/j.meegid.2011.08.013.

2. Tempelis CH, Reeves WC, Bellamy RE, Lofy MF. A Three-Year Study of the Feeding Habits of Culex Tarsalis in Kern County, California*. The American Journal of Tropical Medicine and Hygiene. 1965;14(1):170-7. doi: 10.4269/ajtmh.1965.14.170.

3. Turell MJ, Dohm DJ, Sardelis MR, O'guinn ML, Andreadis TG, Blow JA. An Update on the Potential of North American Mosquitoes (Diptera: Culicidae) to Transmit West Nile Virus. Journal of Medical Entomology. 2005;42(1):57-62. doi: 10.1093/jmedent/42.1.57.

4. (CDC) CfDC. Saint Louis Encephalitis | Transmission 2018 [cited 2020 March 16]. Available from: https://www.cdc.gov/sle/technical/transmission.html.

570 5. Scott JG, Yoshimizu MH, Kasai S. Pyrethroid resistance in Culex pipiens
571 mosquitoes. Pesticide Biochemistry and Physiology. 2015;120:68-76. doi:
572 10.1016/j.pestbp.2014.12.018.
573 6. (CDPH). CDoPH. Latest West Nile Activity in California 2020. Available from:
574 http://westnile.ca.gov/.
575 7. (CDC). CfDCaP. Saint Louis Encephalitis | Statistics & Maps 2019 [cited 2020
576 March 16]. Available from: https://www.cdc.gov/sle/technical/epi.html.
577 8. Costa LG. Chapter 9 - The neurotoxicity of organochlorine and pyrethroid
578 pesticides. In: Lotti M, Bleecker ML, editors. Handbook of Clinical Neurology. 131:
579 Elsevier; 2015. p. 135-48.
580 9. Zhorov BS, Dong K. Elucidation of pyrethroid and DDT receptor sites in the
581 voltage-gated sodium channel. NeuroToxicology. 2017;60:171-7. doi:
582 https://doi.org/10.1016/j.neuro.2016.08.013.
583 10. Dong K, Du Y, Rinkevich F, Nomura Y, Xu P, Wang L, et al. Molecular Biology of
584 Insect Sodium Channels and Pyrethroid Resistance. Insect Biochemistry and Molecular
585 Biology. 2014;50:1-17. doi: 10.1016/j.ibmb.2014.03.012.
586 11. Yoshimizu MH, Padgett K, Kramer V. Surveillance of a kdr Resistance Mutation
587 in Culex pipiens (Diptera: Culicidae) and Culex quinquefasciatus in California. Journal of
588 Medical Entomology. 2020. doi: 10.1093/jme/tjz208.
589 12. Davies TGE, Field LM, Usherwood PNR, Williamson MS. DDT, pyrethrins,
590 pyrethroids and insect sodium channels. IUBMB Life. 2007;59(3):151-62. doi:
591 10.1080/15216540701352042.

592 13. Brogden W, Chan A. Guideline for Evaluating Insecticide Resistance in Vectors
593 Using the CDC Bottle Bioassay. Retrieved from
594 http://www.cdc.gov/malaria/resources/pdf/fsp/ir_manual/ ir_cdc_bioassay_en.pdf. 2012.
595 14. Reid MC, McKenzie FE. The contribution of agricultural insecticide use to
596 increasing insecticide resistance in African malaria vectors. Malaria Journal.
597 2016;15(1):107. doi: 10.1186/s12936-016-1162-4.
598 15. Hien A, Soma D, Hema O, Bayili B, Namountougou M, Gnankiné O, et al.
599 Evidence that agricultural use of pesticides selects pyrethroid resistance within
600 Anopheles gambiae s.l. populations from cotton growing areas in Burkina Faso, West
601 Africa. PLoS ONE 12(3): e0173098. https://doi.org/10.1371/journal.pone.0173098.
602 2017.
603 16. Elnaiem D-EA, Kelley K, Wright S, Laffey R, Yoshimura G, Reed M, et al. Impact
604 of Aerial Spraying of Pyrethrin Insecticide on Culex pipiens and Culex tarsalis (Diptera:
605 Culicidae) Abundance and West Nile Virus Infection Rates in an Urban/Suburban Area
606 of Sacramento County, California. Journal of Medical Entomology. 2008;45(4):751-7.
607 doi: 10.1093/jmedent/45.4.751.
608 17. Reisen WK, Carroll BD, Takahashi R, Fang Y, Garcia S, Martinez VM, et al.
609 Repeated West Nile Virus Epidemic Transmission in Kern County, California, 2004–
610 2007. Journal of Medical Entomology. 2009;46(1):139-57. doi: 10.1603/033.046.0118.
611 18. Vanlandingham DL, Schneider BS, Klingler K, Fair J, Beasley D, Huang J, et al.
612 REAL-TIME REVERSE TRANSCRIPTASE?POLYMERASE CHAIN REACTION
613 QUANTIFICATION OF WEST NILE VIRUS TRANSMITTED BY CULEX PIPIENS

614 QUINQUEFASCIATUS. The American Journal of Tropical Medicine and Hygiene Am J
615 Trop Med Hyg. 2004;71(1):120-3. doi: 10.4269/ajtmh.2004.71.120.
616 19. Batson J, Dudas G, Haas-Stapleton E, Kistler AL, Li LM, Logan P, et al. Single
617 mosquito metatranscriptomics identifies vectors, emerging pathogens and reservoirs in
618 one assay. bioRxiv. 2020:2020.02.10.942854. doi: 10.1101/2020.02.10.942854.
619 20. Amweg EL, Weston DP, You J, Lydy MJ. Pyrethroid Insecticides and Sediment
620 Toxicity in Urban Creeks from California and Tennessee. Environmental Science &
621 Technology. 2006;40(5):1700-6. doi: 10.1021/es051407c.
622 21. Nkya TE, Akhouayri I, Kisinza W, David J-P. Impact of environment on mosquito
623 response to pyrethroid insecticides: Facts, evidences and prospects. Insect
624 Biochemistry and Molecular Biology. 2013;43(4):407-16. doi:
625 10.1016/j.ibmb.2012.10.006.
626 22. Brogdon WGC, A., editor Guideline for Evaluating Insecticide Resistance in
627 Vectors Using the CDC Bottle Bioassay2012 2012.
628 23. Bolger AM, Lohse M, Usadel B. Trimmomatic: a flexible trimmer for Illumina
629 sequence data. Bioinformatics. 2014;30(15):2114-20. doi:
630 10.1093/bioinformatics/btu170.
631 24. Bankevich A, Nurk S, Antipov D, Gurevich AA, Dvorkin M, Kulikov AS, et al.
632 SPAdes: A New Genome Assembly Algorithm and Its Applications to Single-Cell
633 Sequencing. Journal of Computational Biology. 2012;19(5):455-77. doi:
634 10.1089/cmb.2012.0021.
635 25. Langmead B, Salzberg SL. Fast gapped-read alignment with Bowtie 2. Nature
636 Methods. 2012;9(4):357-9. doi: 10.1038/nmeth.1923.

637 26. Untergasser A, Cutcutache I, Koressaar T, Ye J, Faircloth BC, Remm M, et al.
638 Primer3—new capabilities and interfaces. Nucleic Acids Research. 2012;40(15):e115-e.
639 doi: 10.1093/nar/gks596.
640 27. BLAST: Basic Local Alignment Search Tool.
641 28. Chen L, Zhong D, Zhang D, Shi L, Zhou G, Gong M, et al. Molecular Ecology of
642 Pyrethroid Knockdown Resistance in Culex pipiens pallens Mosquitoes. PLOS ONE.
643 2010;5(7). doi: 10.1371/journal.pone.0011681.
644 29. Edgar RC. MUSCLE: multiple sequence alignment with high accuracy and high
645 throughput. Nucleic Acids Research. 2004;32(5):1792-7. doi: 10.1093/nar/gkh340.
646 30. Venables WNR, B. D. . Moderm Applied Statistics with S. 4 ed. Springer, New
647 York2002.
648 31. Team RC. R: A language and environment for statistical computing Vienna,
649 Austria2019. Available from: https://www.R-project.org/.
650 32. Wickham H. ggplot2: Elegant Graphics for Data Analysis. Springer-Verlag New
651 York2016.
652 33. Tang W, Wang D, Wang J, Wu Z, Li L, Huang M, et al. Pyrethroid pesticide
653 residues in the global environment: An overview. Chemosphere. 2018;191:990-1007.
654 doi: 10.1016/j.chemosphere.2017.10.115.
655 34. WHO, Organizaiton WH. Test procedures for insecticide resistance monitoring in
656 malaria vector mosquitoes (Second edition). Retrieved from
657 https://apps.who.int/iris/bitstream/handle/10665/250677/9789241511575-eng.pdf. 2018.
658 35. Zhou L, Lawrence GG, Vineis JH, McAllister JC, Wirtz RA, Brogdon WG.
659 Detection of Broadly Distributed Sodium Channel Alleles Characteristic of Insect

660 Pyrethroid Resistance in West Nile Virus Vector Culex pipiens Complex Mosquitoes in
661 the United States. Journal of Medical Entomology. 2009;46(2):321-7. doi:
662 10.1603/033.046.0217.
663 36. Mischke T. Agricultural sources of DDT residues in California's environment.
664 1985.
665 37. Maignan M, Viglino D, Hablot M, Masson NT, Lebeugle A, Muret RC, et al.
666 Diagnostic accuracy of a rapid RT-PCR assay for point-of-care detection of influenza
667 A/B virus at emergency department admission: A prospective evaluation during the
668 2017/2018 influenza season. PLOS ONE. 2019;14(5):e0216308. doi:
669 10.1371/journal.pone.0216308.
670 38. Saingamsook J, Saeung A, Yanola J, Lumjuan N, Walton C, Somboon P. A
671 multiplex PCR for detection of knockdown resistance mutations, V1016G and F1534C,
672 in pyrethroid-resistant Aedes aegypti. Parasites & Vectors. 2017;10(1):465. doi:
673 10.1186/s13071-017-2416-x.
674 39. Cornel AJ, McAbee RD, Rasgon J, Stanich MA, Scott TW, Coetzee M.
675 Differences in Extent of Genetic Introgression Between Sympatric Culex pipiens and
676 Culex quinquefasciatus (Diptera: Culicidae) in California and South Africa. Journal of
677 Medical Entomology. 2003;40(1):36-51. doi: 10.1603/0022-2585-40.1.36.
678 40. Tietze NS, Stephenson, M. F., Sidhom, N. T., & Binding, P. L. Mark-recapture of
679 *Culex erythrothorax* in Santa Cruz County, California. J Am Mosq Control Assoc.
680 2003;19(2):134-8.

681 41. Workman PD, Walton, W. E. Emergence patterns of *Culex* mosquitoes at an
682 experimental constructed treatment wetland in southern California. J Am Mosq Control
683 Assoc. 2000;16(2):124-30.
684 42. Weston DP, Holmes RW, You J, Lydy MJ. Aquatic Toxicity Due to Residential
685 Use of Pyrethroid Insecticides. Environmental Science & Technology.
686 2005;39(24):9778-84. doi: 10.1021/es0506354.
687 43. Roos C, Uunk EJB. Effects of stormwater sewer discharges on the aquatic
688 community in urban canals in Lelystad. Hydrobiological Bulletin. 1987;21(2):207-12. doi:
689 10.1007/BF02255446.
690 44. Diabaté A, Baldet T, Chandre F, Akoobeto M, Guiguemdé TR, Darriet F, et al.
691 The role of agricultural use of insecticides in resistance to pyrethroids in Anopheles
692 gambiae s.l. in Burkina Faso. The American journal of tropical medicine and hygiene.
693 2002;67 6:617-22.
694 45. Yadouléton A, N'Guessan R, Allagbé H, Asidi A, Boko M, Osse R, et al. The
695 impact of the expansion of urban vegetable farming on malaria transmission in major
696 cities of Benin. Parasites & Vectors. 2010;3(1):118. doi: 10.1186/1756-3305-3-118.
697 46. Scott JG. Cytochromes P450 and insecticide resistance. Insect Biochemistry and
698 Molecular Biology. 1999;29(9):757-77. doi: 10.1016/S0965-1748(99)00038-7.
699 47. Howard TS, Novak MG, Kramer VL, Bronson LR. Public health pesticide use in
700 California: a comparative summary. J Am Mosq Control Assoc. 2010;26(3):349-53. doi:
701 10.2987/10-5997.1.
702 48. Macoris MdL, Martins AJ, Andrighetti MTM, Lima JBP, Valle D. Pyrethroid
703 resistance persists after ten years without usage against Aedes aegypti in governmental

704 campaigns: Lessons from São Paulo State, Brazil. PLoS Negl Trop Dis. 2018;12(3). doi:

705 10.1371/journal.pntd.0006390.

706

Figure 1

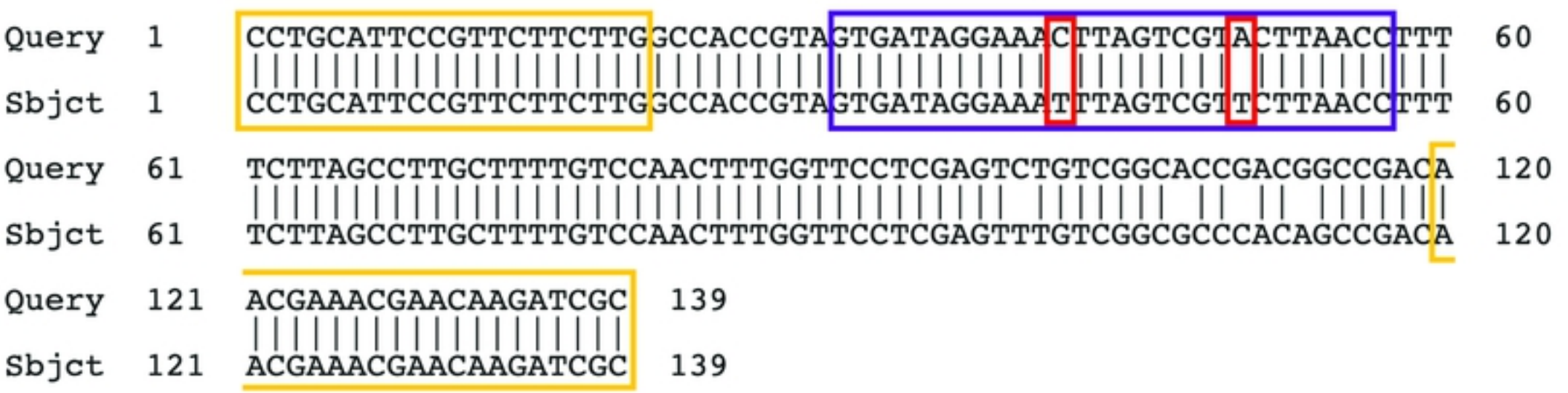

Figure 2

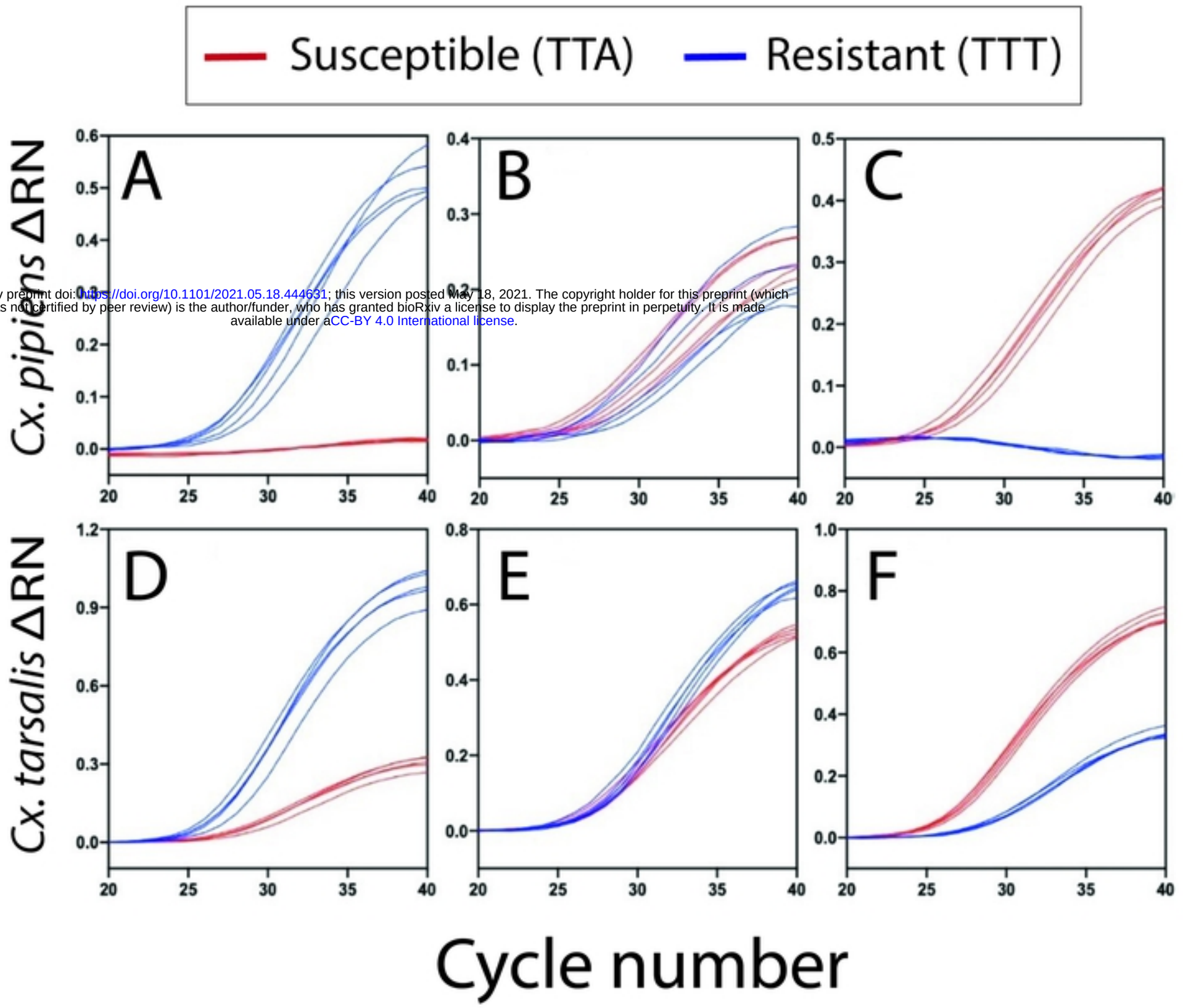

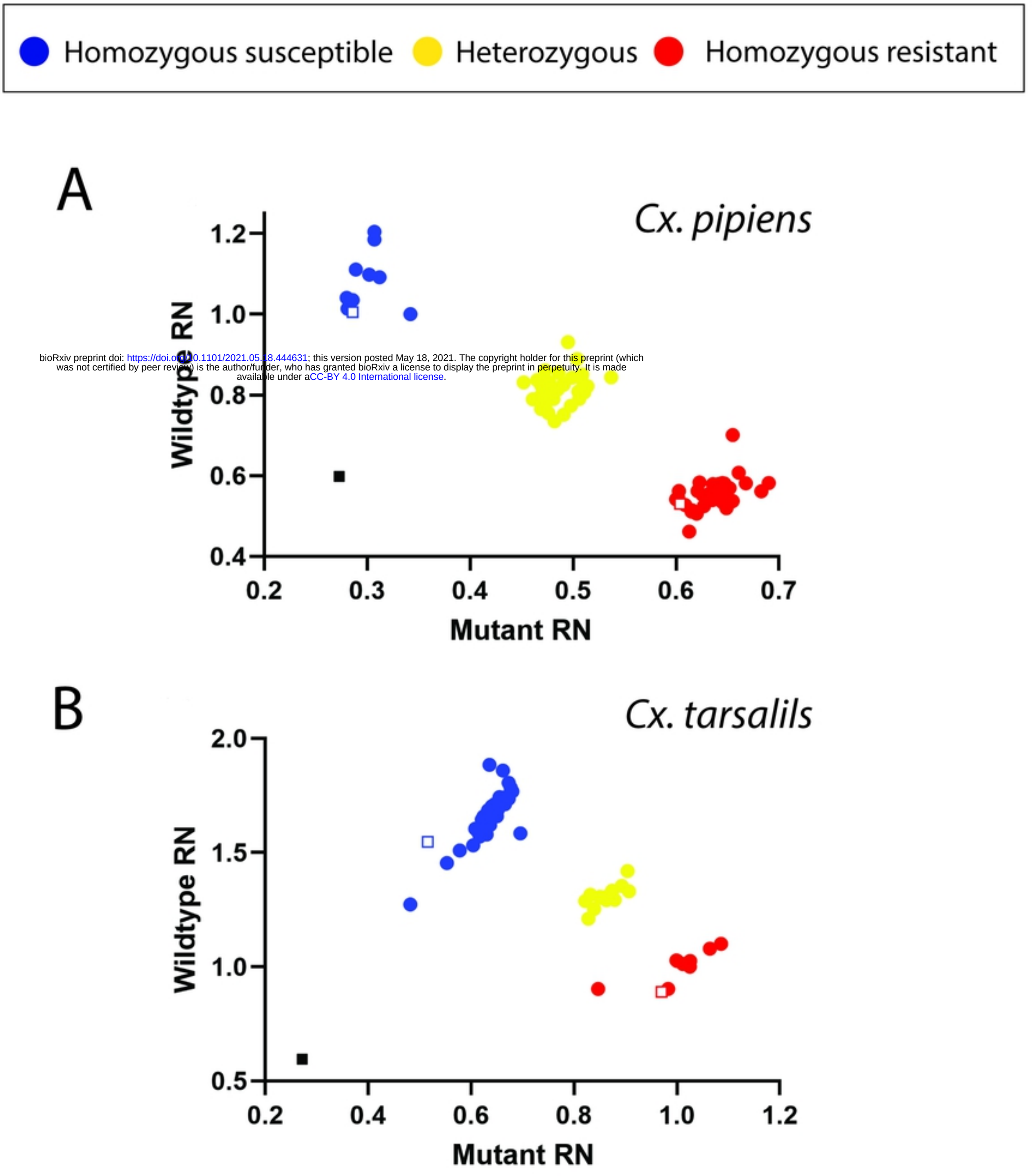

Figure 4

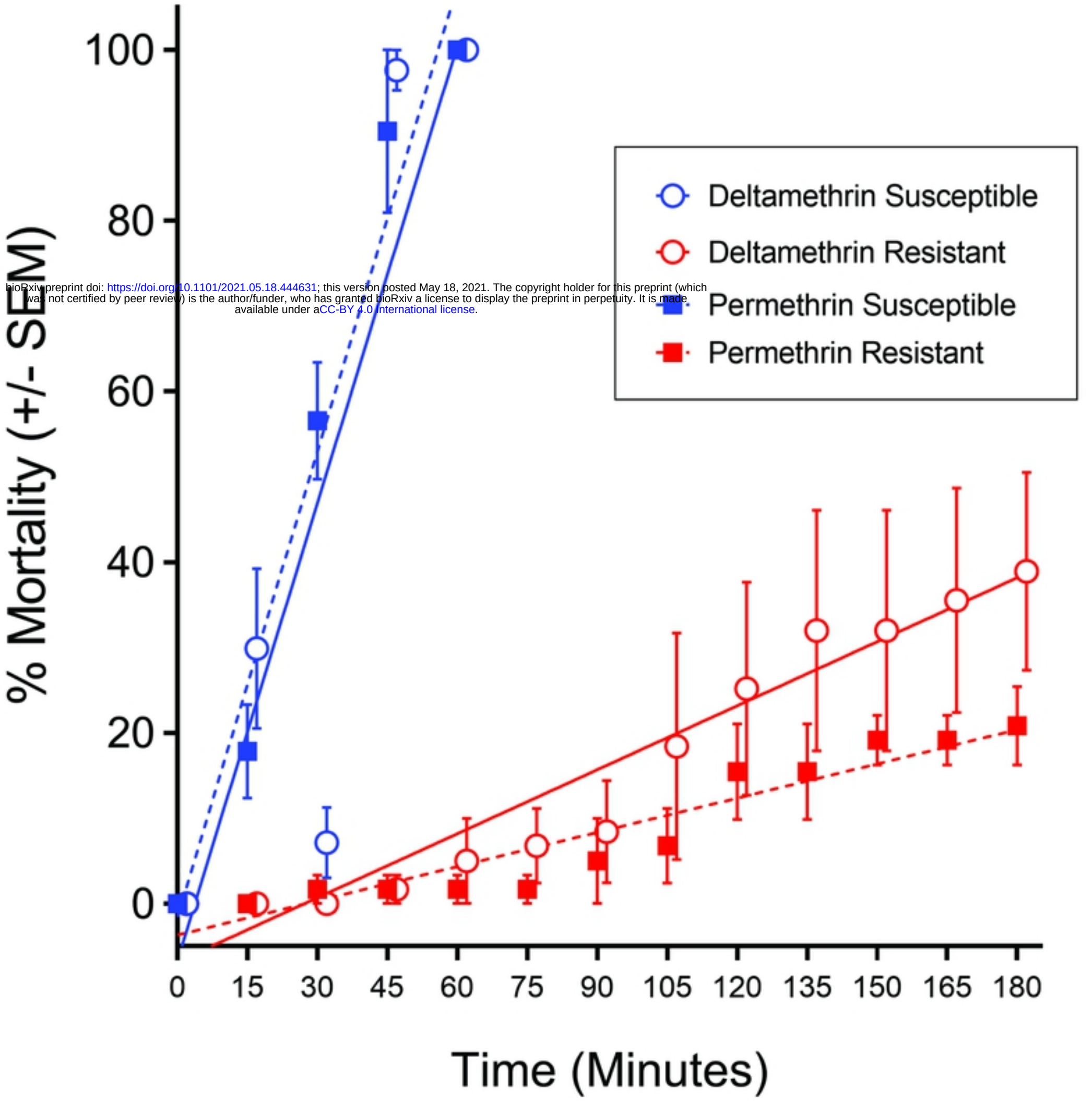

Figure 5

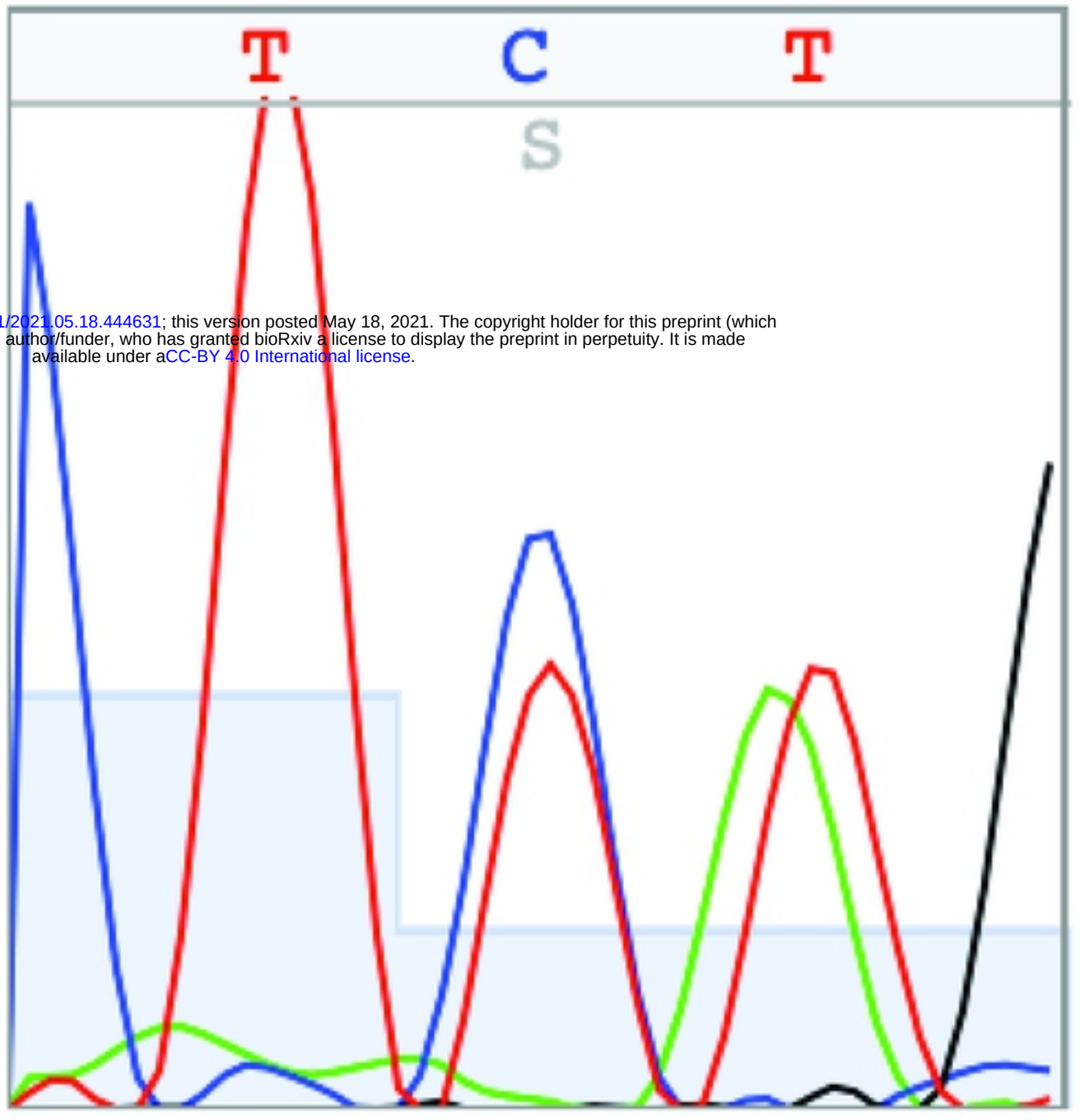

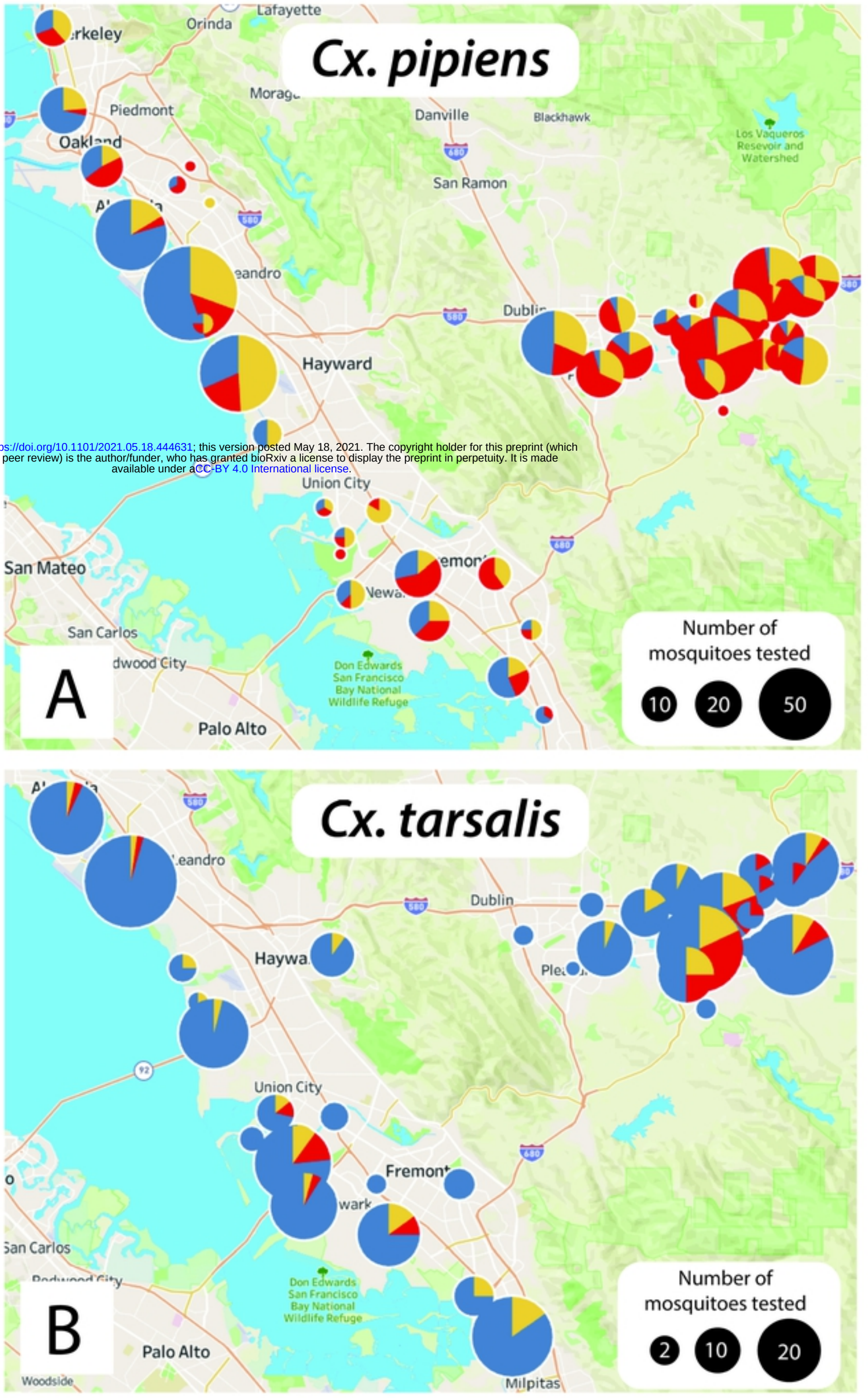

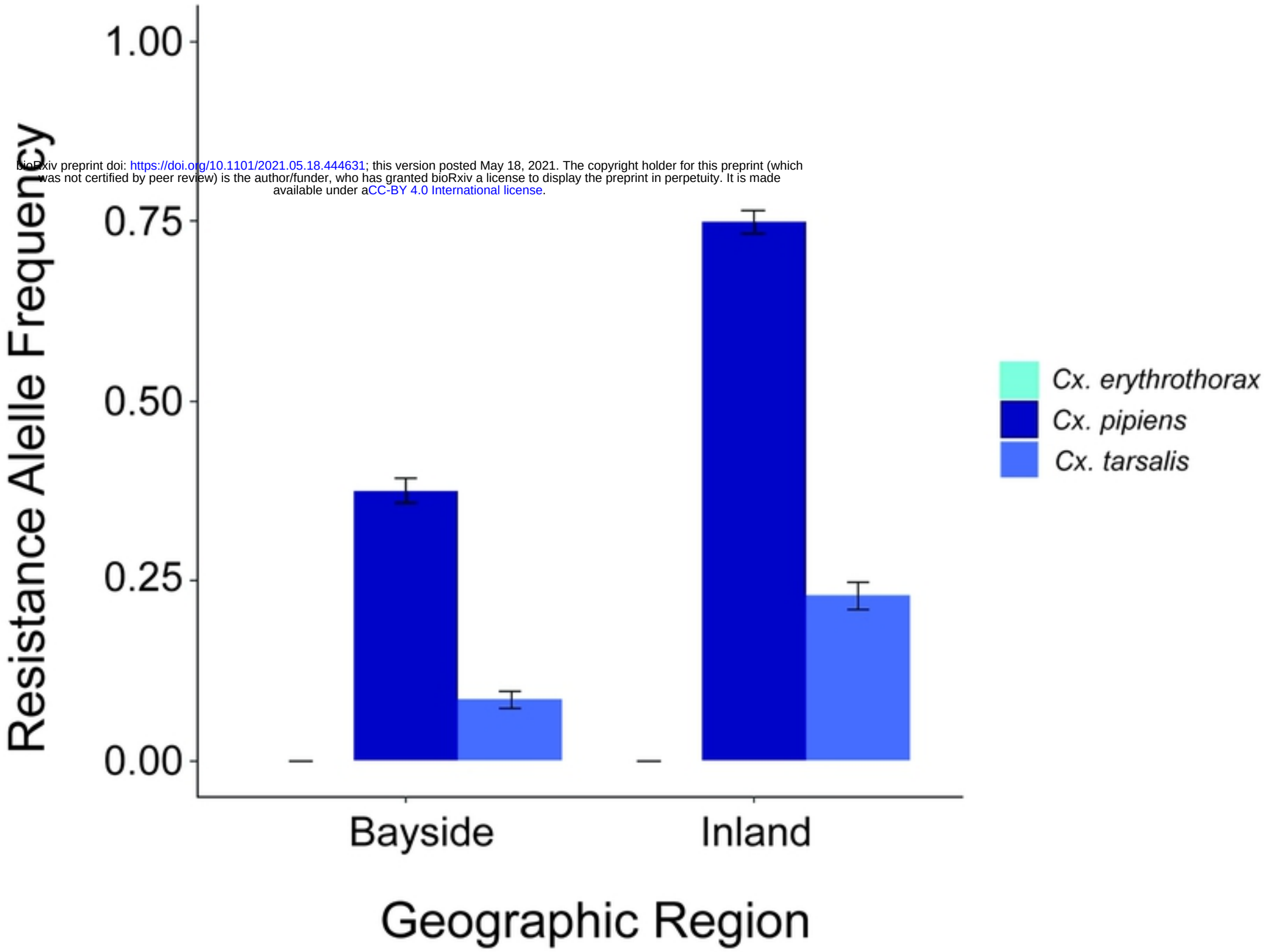

Figure 8